Analytical Methods

ROYAL SOCIETY OF CHEMISTRY

CRITICAL REVIEW

View Article Online
View Journal | View Issue

Cite this: *Anal. Methods*, 2025, **17**, 2235

3D-printed electrodes for electrochemical detection of environmental analytes

Liangliang Pan,[ab] Shijing Zhou,[b] Jiaying Yang,[b] Tongyun Fei,[b] Shuduan Mao,*[b] Li Fu *[c] and Cheng-Te Lin [def]

Environmental monitoring faces increasing demands for rapid, sensitive, and cost-effective analytical methods to detect various pollutants. Three-dimensional (3D) printing technology has emerged as a transformative approach for fabricating electrochemical sensors, offering unprecedented flexibility in electrode design and potential for customization. This comprehensive review examines recent advances in 3D-printed electrochemical sensors for environmental analysis, focusing on manufacturing technologies, materials development, and surface modification strategies. We analyze various printing approaches, including fused deposition modeling, stereolithography, and selective laser melting, discussing their relative advantages and limitations for electrode fabrication. The review explores conductive materials development, from carbon-based composites to novel metal-containing filaments, and examines crucial surface modification techniques that enhance sensor performance. Key applications in environmental monitoring are evaluated, including the detection of heavy metals, pathogens, antibiotics, and organophosphates, with particular attention to analytical performance metrics and real-world applicability. Technical challenges are critically assessed, including limitations in printing resolution, material conductivity, and long-term stability. The review concludes by identifying promising research directions, such as the integration of advanced materials and the development of automated manufacturing processes, highlighting opportunities for improving sensor performance and commercial viability in environmental monitoring applications.

Received 19th December 2024
Accepted 20th February 2025

DOI: 10.1039/d4ay02271h

rsc.li/methods

Introduction

Environmental pollution poses significant challenges to human health and ecosystem stability, driven by the increasing discharge of diverse chemical pollutants from industrial, agricultural, and urban activities.[1,2] These contaminants, ranging from heavy metals and organic compounds to emerging pollutants, often exist at trace levels in environmental matrices yet can exert profound toxic effects.[3] The ability to detect and quantify these pollutants accurately and rapidly is crucial for environmental monitoring and regulatory compliance.[4] Traditional analytical techniques, while precise, typically require sophisticated instrumentation, specialized expertise, and lengthy sample preparation procedures, limiting their application for routine monitoring and on-site analysis.[5,6] In recent years, electrochemical sensors have emerged as promising alternatives for environmental analysis due to their high sensitivity, good selectivity, rapid response, and potential for miniaturization. These advantages, coupled with relatively low cost and simple operation, make electrochemical sensing particularly attractive for developing portable analytical devices.[7,8] However, conventional electrode fabrication methods often involve complex procedures, require expensive materials, and may lack reproducibility in mass production. This has driven the search for new manufacturing approaches that can overcome these limitations while maintaining or enhancing analytical performance.[9,10]

Three-dimensional (3D) printing technology has revolutionized manufacturing across various fields, including analytical chemistry, by enabling the rapid fabrication of complex geometries with high precision and reproducibility.[11] The application of 3D printing in electrochemical sensor development represents a significant advancement, offering unprecedented flexibility in electrode design and the potential for customization based on specific analytical requirements.[12,13] This approach allows for the creation of complete analytical devices that

[a]*College of Environment, Zhejiang University of Technology, Huzhou 313299, China*
[b]*Interdisciplinary Research Academy, Zhejiang Shuren University, Hangzhou 310015, China. E-mail: maoshuduan@zjsru.edu.cn*
[c]*College of Materials and Environmental Engineering, Hangzhou Dianzi University, Hangzhou, 310018, China. E-mail: fuli@hdu.edu.cn*
[d]*Qianwan Institute, Ningbo Institute of Materials Technology and Engineering (NIMTE), Chinese Academy of Sciences, Ningbo, PR China*
[e]*Center of Materials Science and Optoelectronics Engineering, University of Chinese Academy of Sciences, Beijing 100049, China*
[f]*Key Laboratory of Advanced Marine Materials, Ningbo Institute of Materials Technology and Engineering (NIMTE), Chinese Academy of Sciences, Ningbo 315201, China*

integrate sample handling, preparation, and detection components in a single platform.

The versatility of 3D printing technologies in electrode fabrication stems from several key advantages. First, it enables the production of electrodes with complex geometries that would be difficult or impossible to achieve through traditional manufacturing methods.[14] This geometric freedom allows for optimization of electrode surface area, enhancement of mass transport, and integration of multiple functionalities within a single device.[15] Second, 3D printing offers excellent control over the internal structure of electrodes, enabling the creation of porous architectures that can enhance sensitivity and improve analytical performance.[16] Third, the ability to rapidly prototype and modify designs facilitates iterative optimization of electrode configurations for specific applications.[17] Among various 3D printing technologies, fused deposition modeling (FDM) has gained particular attention for electrochemical sensor fabrication due to its accessibility, low cost, and compatibility with a wide range of materials. FDM utilizes thermoplastic filaments containing conductive materials, such as carbon black (CB), graphene, or metal particles, to create electrodes through layer-by-layer deposition.[18,19] The printing parameters, including temperature, speed, and layer height, significantly influence the electrical and electrochemical properties of the resulting electrodes. Understanding and optimizing these parameters is crucial for achieving optimal sensor performance. The development of conductive materials for 3D printing represents another critical aspect of this field. Commercial filaments typically combine thermoplastic polymers like polylactic acid (PLA) or acrylonitrile butadiene styrene (ABS) with conductive additives.[20] While these materials offer adequate conductivity for many applications, there is ongoing research to develop new composites with enhanced electrical properties, improved mechanical strength, and better printing characteristics. This includes the exploration of novel carbon-based materials, metal–organic frameworks, and hybrid composites. Surface modification strategies play a vital role in optimizing the performance of 3D-printed electrodes.[21] Various approaches, including electrochemical activation, chemical treatment, and nanomaterial modification, have been developed to enhance electron transfer kinetics, increase active surface area, and improve sensitivity toward specific analytes.[22] These modifications can also introduce selective recognition elements or catalytic sites for particular environmental contaminants.

The application of 3D-printed electrochemical sensors in environmental analysis has demonstrated promising results across various domains. These include the detection of heavy metals in water samples, monitoring of organic pollutants in soil and sediments, and analysis of pesticides in agricultural runoff. The ability to customize electrode designs for specific analytical challenges, combined with the potential for rapid prototyping and optimization, makes 3D-printed sensors particularly valuable for environmental monitoring applications. Despite these advances, several challenges remain in the development and implementation of 3D-printed electrochemical sensors. These include the need for improved material properties, better understanding of structure–function relationships, and development of standardized fabrication protocols. Additionally, ensuring long-term stability, reproducibility, and reliable performance under field conditions requires further investigation.

In recent years, several comprehensive reviews have explored 3D printing for electrochemical applications, providing valuable overviews of emerging fabrication methodologies and early demonstrations of printed sensors.[23,24] Notably, Ambrosi and Pumera[23] systematically delineated various additive manufacturing platforms for electrochemical devices, emphasizing the fundamental science and first-generation sensor designs. Goh *et al.*[24] further highlighted the potential of printed electrodes for electrochemical impedance spectroscopy applications, including fouling detection in membrane processes. While these works establish the scientific basis for 3D-printed electrochemical systems, relatively few reviews connect these technologies to a broad range of urgent environmental challenges and provide detailed comparisons of the latest material innovations (*e.g.*, nanocomposites, MOFs) for sensor performance.

In this review, we thus aim to bridge these gaps by critically evaluating state-of-the-art 3D printing methods for environmental electrochemical sensing and pollutant detection, examining fundamental fabrication principles as well as advanced electrode compositions. Particular attention is paid to comparing printing strategies for tailoring electrode surface area, conductivity, and selectivity—factors crucial for quantifying trace levels of emerging contaminants. We also address key aspects of sensor reliability, long-term stability, and reproducibility, vital for future field deployment. By highlighting recent progress and outstanding challenges, we provide a roadmap for leveraging 3D-printing technologies to advance next-generation environmental electroanalysis.

3D printing technologies for electrode fabrication

The fabrication of electrochemical sensors through 3D printing technologies has revolutionized the field of analytical chemistry by enabling rapid prototyping and customization of electrode designs. Several printing approaches have emerged as viable methods for electrode fabrication, each offering distinct advantages and limitations for electrochemical applications.

Fused deposition modeling (FDM)

FDM represents the most widely adopted approach for fabricating electrochemical sensors due to its accessibility, cost-effectiveness, and operational simplicity. This dominance stems from its accessibility, cost-effectiveness, and operational simplicity. According to recent literature analysis, FDM significantly outperforms other material extrusion techniques like direct ink writing (DIW), representing more than 68% of published works in the field.[25,26] The technique operates by extruding thermoplastic filaments through a heated nozzle, depositing material layer by layer to construct the desired

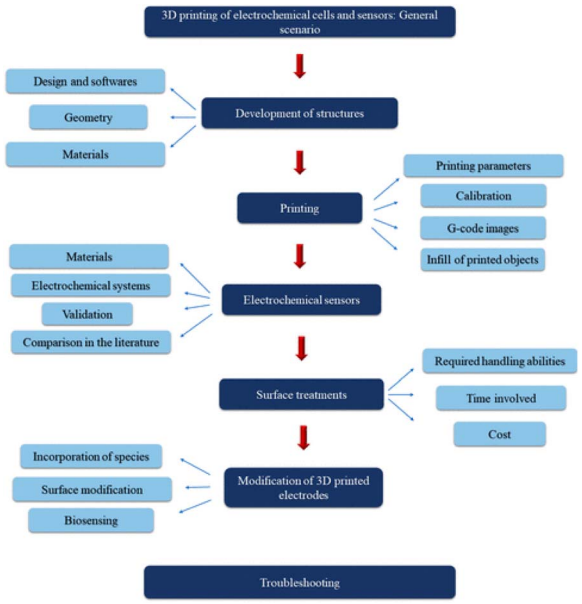

Fig. 1 Scheme of the main steps to follow in the development of 3D printing electrochemical sensors or cells.[27] Copyright, American Chemical Society.

electrode structure. As shown in Fig. 1, the comprehensive process involves multiple stages, from initial design and structure development to final surface treatments and modification steps. The process begins with heating the filament to a semi-molten state, followed by precise deposition onto a building platform where it rapidly solidifies, forming strong bonds between successive layers. This layered construction approach allows for remarkable design freedom, enabling the creation of complex geometries and integrated features that would be challenging or impossible to achieve through traditional manufacturing methods.[28,29]

FDM's popularity in electrochemical sensor development stems from its compatibility with conductive thermoplastic composites, particularly those incorporating carbon-based materials. Commercial filaments typically contain around 8–10% conductive materials (such as graphene or CB) dispersed within a polymer matrix, most commonly PLA.[30,31] The technique allows for the creation of electrodes with layer thicknesses typically ranging from 0.1 to 0.4 mm, providing sufficient resolution for most sensing applications. However, the surface finish of FDM-printed electrodes often requires post-processing due to the inherent roughness created by the layer-by-layer deposition process. As illustrated in Fig. 2, various surface treatment protocols have been developed to enhance the electrochemical performance of printed electrodes, including mechanical polishing, chemical treatment, and electrochemical activation steps. These treatments are crucial for exposing the conductive components and improving electron transfer kinetics at the electrode surface.[32–34] The optimization of printing parameters, such as layer height, printing orientation, and extrusion temperature, also plays a vital role in determining the final electrode performance, with recent studies demonstrating significant improvements in conductivity and electrochemical response through careful parameter control.[32,35,36]

The technique's primary advantage lies in its ability to utilize commercially available conductive filaments, such as CB/PLA or graphene/PLA composites, making it highly accessible to research laboratories. The recent development of lab-made filaments with higher conductive material loadings (up to 40 wt%) has further expanded the capabilities of FDM-printed sensors.[37] Additionally, FDM enables the simultaneous printing of conductive and non-conductive materials through dual-extruder systems, facilitating the fabrication of complete electrochemical cells and integrated sensing platforms. This versatility has led to numerous innovative applications, from simple three-electrode systems to complex microfluidic devices integrated with multiple sensing elements.[18,38,39] Recent studies have demonstrated the successful application of FDM-printed electrodes in various analytical tasks, including heavy metal detection,[40] biomolecule sensing,[37] and environmental monitoring.[39] The ability to rapidly prototype and modify designs, coupled with the low cost of materials and equipment, has made FDM an indispensable tool in modern electroanalytical chemistry. The technology has evolved to address various challenges, such as improving electrode conductivity through surface treatments and developing new composite materials, while maintaining its fundamental advantages of accessibility and ease of use. Furthermore, the integration of FDM-printed electrodes with other analytical techniques and the development of multi-material printing approaches continue to expand the possibilities for creating more sophisticated and capable sensing platforms.[17,41,42]

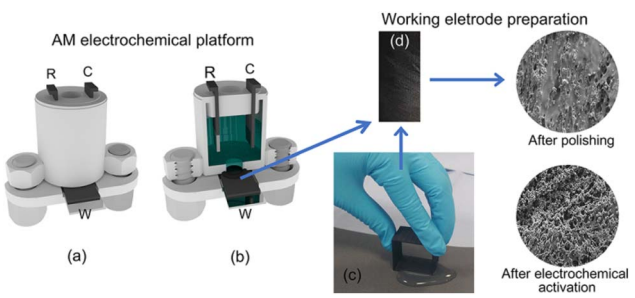

Fig. 2 Schematic representation of an efficient and commonly employed pretreatment performed on a CB/PLA 3D printed electrode.[29] Copyright, American Chemical Society.

Stereolithography (SLA)

Stereolithography offers an alternative approach to electrode fabrication, utilizing photopolymerization to create highly precise structures. The process involves selectively curing liquid photopolymer resins using ultraviolet light, either through direct laser writing or digital light projection. SLA provides exceptional resolution, capable of producing features between 25 and 100 micrometers, significantly finer than what is achievable with FDM.

The superior surface finish and precision of SLA make it particularly valuable for applications requiring intricate electrode geometries or microfluidic integration. However, the

limitation in available conductive photopolymer resins poses a significant challenge for direct electrode printing. Consequently, SLA is often employed to create electrode substrates or housing structures, which are subsequently modified with conductive materials through various post-processing techniques.

SLA's layer thickness typically ranges from 0.05 to 0.15 mm, enabling the creation of smooth surfaces that require minimal post-processing. The technique's ability to produce isotropic structures also offers advantages in terms of mechanical properties and structural integrity, though the restricted range of printable materials currently limits its widespread adoption in electrochemical sensor fabrication.

Selective laser melting (SLM)

SLM represents a sophisticated approach to electrode fabrication, particularly for creating precise metallic electrochemical sensors. As demonstrated by Pumera's pioneering work, SLM technology employs high-powered lasers to selectively fuse metal or alloy particles through a layer-by-layer process, where each layer is bonded by heating the particles just above their melting point.[43] The technique's key advantage lies in its ability to produce mechanically robust electrodes with intricate geometries while maintaining excellent electrical conductivity. As shown in Fig. 3A, complex helical-shaped electrodes can be fabricated with high precision, demonstrating the design freedom enabled by SLM technology.[44] The physicochemical properties of the produced electrodes depend critically on several parameters, including the composition and particle size of the metal powder, layer thickness settings, and laser power optimization.[43,44] These parameters must be carefully controlled to ensure consistent electrode performance and reproducibility. For instance, when developing stainless steel electrodes, Ambrosi *et al.*[43] demonstrated that careful control over the precursor metal composition was crucial for achieving uniform electrochemical properties comparable to commercial steel electrodes.

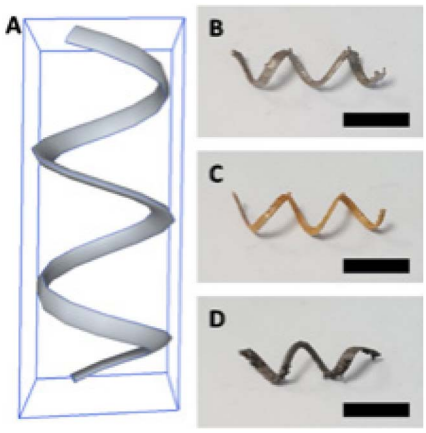

Fig. 3 Scheme of the 3D-printed helical metal electrode and photographs of 3D-printed stainless-steel electrode and after electroplating of gold and bismuth.[44] Copyright, American Chemical Society. Copyright, Wiley.

The versatility of SLM in electrode modification and surface functionalization makes it particularly valuable for developing specialized electrochemical sensors. Fig. 3B–D illustrates how SLM-printed stainless steel electrodes can be modified through electrodeposition of different metals like gold and bismuth to enhance their sensing capabilities. This modification flexibility enables the creation of electrodes tailored for specific analytical applications. For example, gold-modified SLM electrodes have demonstrated superior sensitivity in detecting nitroaromatic compounds, achieving detection limits 4.5 times lower than conventional glassy carbon electrodes.[44] The technique has also proven effective for fabricating electrochemical biosensors, as demonstrated by the development of DNA sensors using gold-plated SLM electrodes, where the strong interaction between electroplated gold and thiol groups of DNA recognition elements enabled sensitive detection of target DNA sequences.[45] The ability to precisely control the internal and surface structure of SLM-printed electrodes has led to developments in various applications, from environmental monitoring to clinical diagnostics.

Despite its advantages, SLM technology faces several practical limitations that currently restrict its widespread adoption in electrochemical sensor development. The most significant barrier is the high cost of SLM equipment, with prices approximately 200 times higher than conventional FDM 3D printers.[43,45] Additionally, the metal powders used as printing materials require special handling procedures and represent a significant ongoing cost. The technique demands sophisticated control over numerous printing parameters to prevent defects and ensure consistent electrical properties throughout the printed structure. These challenges have led researchers to explore alternative approaches, such as FDM printing with conductive filaments, for more accessible electrode fabrication. However, for applications requiring superior mechanical properties and precise control over electrode geometry, SLM remains unmatched. The success of SLM in producing functional electrochemical devices has been demonstrated through various applications, including pH sensing,[43] heavy metal detection,[46] and biosensing platforms,[47] suggesting that as the technology becomes more accessible, it may play an increasingly important role in the future of electrochemical sensor fabrication.

3D electronic printing methods for electrode fabrication

While FDM and other conventional additive manufacturing techniques have dominated the development of printed electrodes, 3D electronic printing methods such as aerosol jet printing and inkjet printing are increasingly recognized for their precise material deposition and design flexibility.[48,49] Aerosol jet printing, for example, employs a tightly focused aerosol stream to deposit functional inks onto substrates of varying geometries. This approach enables high-resolution patterning of conductive, semiconductive, or dielectric inks directly onto conformal and three-dimensional surfaces. Inkjet printing likewise offers a non-contact, digitally controlled process that can deposit low-viscosity conductive nanoparticles or polymer inks in fine droplets, allowing the fabrication of microscale features.

These printing methodologies are especially relevant for electrode fabrication, as they facilitate the controlled deposition of metal nanoparticles (*e.g.*, silver, copper) or carbon-based materials (*e.g.*, graphene, carbon nanotubes), thereby improving the electrode's electrical conductivity and overall sensing performance. Recent reviews have highlighted how aerosol jet and inkjet-printed electrodes can be functionalized to detect heavy metals, pesticides, and organic pollutants in environmental applications, while also enabling integration of multiple sensor layers with minimal post-processing.[50–52] As 3D electronic printing continues to advance, new formulations (including biocompatible or stretchable inks) and scalable manufacturing protocols are expected to broaden the scope of additively manufactured electrodes for environmental electroanalysis.

Comparison of printing approaches

Each printing technology offers distinct advantages and limitations for electrode fabrication that significantly impact the final device performance and manufacturing process. FDM stands out for its accessibility, cost-effectiveness, and office-friendly operation environment. For instance, Maurel *et al.*[53] demonstrated electrode filaments with highly loaded active materials using a PLA/graphite/carbon-black configuration. The main limitation of FDM lies in its relatively low electrical conductivity due to the necessary use of thermoplastic polymers as binding materials.[54] This challenge can be partially addressed through optimization of conductive material loading, though this affects printability and mechanical properties. SLA excels in producing high-resolution structures with excellent surface finish, particularly valuable for creating complex architectures with precisely controlled features.[54,55] The ability to fabricate truly arbitrary designs without toolpath limitations enables innovative electrode configurations that can enhance electrochemical performance.[56] However, SLA requires photocurable materials and typically demands post-processing steps to achieve conductivity, which can increase manufacturing complexity and cost. Selective Laser Sintering (SLS) provides superior control over material properties through direct powder processing, enabling the fabrication of both metallic and ceramic components with excellent conductivity and mechanical stability.[57] This versatility allows for the integration of current collectors and active materials within the same printing process. As demonstrated by Zhao *et al.*,[58] SLS-fabricated micropillar array electrodes delivered an areal energy density of 2.98×10^{-6} W h cm^{-2}, significantly higher than conventional planar structures. The main drawbacks of SLS include high equipment costs and operational complexity, which can limit its widespread adoption. DIW offers a balance between resolution and material flexibility, allowing for a wide range of printable compositions including active materials, conductivity enhancers, and polymer binders.[59] This versatility has enabled the fabrication of various electrode architectures, from interdigitated structures to 3D scaffolds. For example, Fu *et al.*[60] achieved enhanced electrical conductivity through the incorporation of graphene oxide in electrode inks, with values reaching 31.6 and 6.1 S cm^{-1} for cathode and anode materials respectively. The primary challenge with DIW lies in ink formulation, as materials must exhibit appropriate rheological properties while maintaining desired electrochemical performance. The selection of printing technology ultimately depends on specific application requirements, balancing factors such as resolution, material compatibility, cost, and scalability.

Printing parameters affecting electrode performance

The electrochemical performance of 3D-printed electrodes is heavily influenced by various printing parameters, regardless of the chosen technology. In FDM printing, critical parameters include extrusion temperature, printing speed, layer height, and infill pattern. As shown in Table 1, these parameters directly impact electrode performance – for instance, printing temperature affects the extruded filament flow, which in turn influences the surface quality of the electrode.[18,36] Improper temperature settings can lead to incomplete fusion between layers or excessive material flow, both compromising the electrode's electrochemical response. Research by Rocha *et al.*[18]

Table 1 Critical FDM printing parameters and their impact on electrochemical electrode performance

Parameter	Function in printing process	Impact on electrode performance
Printing temperature	Controls polymer melting and flow characteristics during extrusion	- Affects interfacial bonding between layers - Influences conductivity pathway formation - Determines surface roughness
Platform temperature	Regulates cooling rate and initial layer adhesion	- Influences overall structural integrity - Affects formation of conductive networks - Impacts surface morphology
Print speed	Controls material deposition rate and cooling time	- Affects particle distribution and orientation - Influences layer uniformity - Impacts conductive pathway formation
Layer height	Determines resolution and layer thickness	- Affects surface area and roughness - Influences electron transfer efficiency - Impacts mechanical strength
Infill pattern	Defines internal structure of electrode	- Determines conductive pathway continuity - Affects mechanical stability - Influences active surface area

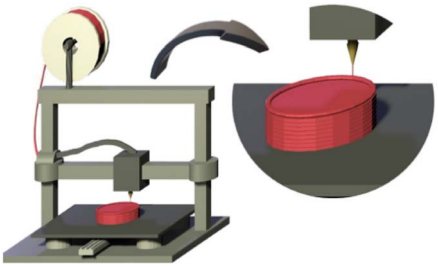

Fig. 4 Illustration of a FDM 3D printer, highlighting in the zoomed-in image the layer-by-layer deposition process, forming the final object.[61] Copyright, MDPI.

demonstrated that printing parameters significantly affect the electrochemical performance of 3D-printed carbon electrodes, with optimal settings yielding enhanced electron transfer rates. The relationship between these parameters is complex – for example, while higher temperatures can improve layer adhesion and conductivity, they may also lead to material degradation if excessive. As illustrated in Fig. 4, the FDM process involves careful control of these parameters during the layer-by-layer deposition to form the final object. The integration of conductive materials within the polymer matrix during printing is particularly crucial, as it determines the formation of conductive pathways essential for electrochemical sensing.

Print orientation emerges as a crucial factor in determining the electrochemical response, particularly for FDM-printed electrodes. According to studies by Bin Hamzah *et al.*,[36] vertical printing orientation often results in improved conductivity due to the alignment of conductive pathways between layers. This alignment is critical because it affects the electron transfer efficiency across the electrode surface. As depicted in Fig. 5, the arrangement of conductive particles within the polymeric matrix creates different types of percolation networks, which directly influence the electrode's performance.[61] The figure clearly shows how various particle arrangements can lead to different conductive pathways, from optimal networks (B) to insufficient connectivity (D). The choice of infill pattern similarly affects both mechanical stability and electrochemical performance. Research by Cardoso *et al.* demonstrated that continuous patterns generally provide better

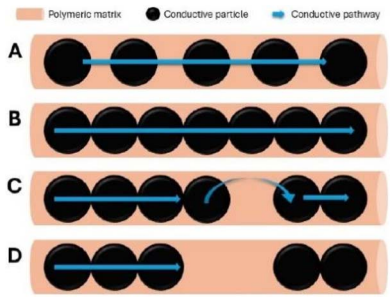

Fig. 5 Illustration of conductive networks with (A) low fraction of conductive particles, (B) the critical value, (C) small gaps, and (D) insufficient conductive material.[61] Copyright, MDPI.

electrical connectivity due to uninterrupted pathways for electron transfer.[25] The internal structure created by different infill patterns can significantly impact the electrode's active surface area and, consequently, its sensitivity toward target analytes. Studies have shown that higher infill densities typically result in better conductivity but must be balanced against other factors such as material usage and printing time.[18,27]

The optimization of these parameters requires careful consideration of the intended application and specific requirements for analytical performance. For instance, slower printing speeds and higher temperatures often result in better layer adhesion and improved conductivity but may affect the dimensional accuracy of the printed structures. Stefano *et al.*[62] demonstrated that optimization of printing parameters could significantly enhance the performance of CB-based conductive filaments for electrochemical sensing applications. The challenge lies in finding the optimal balance – for example, while slower printing speeds can improve layer adhesion and conductivity, they significantly increase manufacturing time and cost.[18] Temperature control is equally critical; studies have shown that maintaining consistent temperature throughout the printing process is essential for achieving uniform electrical properties.[63,64] The relationship between these parameters is often interdependent – for instance, changes in printing speed may require corresponding adjustments in temperature to maintain optimal performance. Research by Kalinke *et al.*[34] demonstrated how surface treatments post-printing could compensate for some parameter-related limitations, highlighting the importance of considering both printing parameters and post-processing steps in electrode development. This optimization process becomes particularly crucial when developing electrodes for specific applications, such as clinical analysis, where reproducibility and sensitivity are paramount.

Materials for 3D-printed electrochemical sensors

Conductive thermoplastic composites

The development of conductive thermoplastic composites represents a transformative advancement in fabricating 3D-printed electrochemical sensors. The fundamental composition involves incorporating electrically conductive materials within an insulating thermoplastic matrix to create printable materials that combine electrical conductivity with mechanical stability. PLA and ABS have emerged as preferred matrix materials due to their optimal printing characteristics, with PLA offering biodegradability and processing temperatures around 230 °C, while ABS provides enhanced mechanical properties and processing flexibility between 200–300 °C.[65] The selection of conductive fillers has primarily focused on carbon-based materials, including CB (16–20 wt%), graphene (20–25 wt%), carbon nanotubes (0.31–3.30 vol%), and graphite microparticles, owing to their high surface area, excellent electrical conductivity, and chemical stability.[66–68] For instance, nanographite-loaded PLA composites have demonstrated effective percolation and high conductivity at 25 wt% loading,

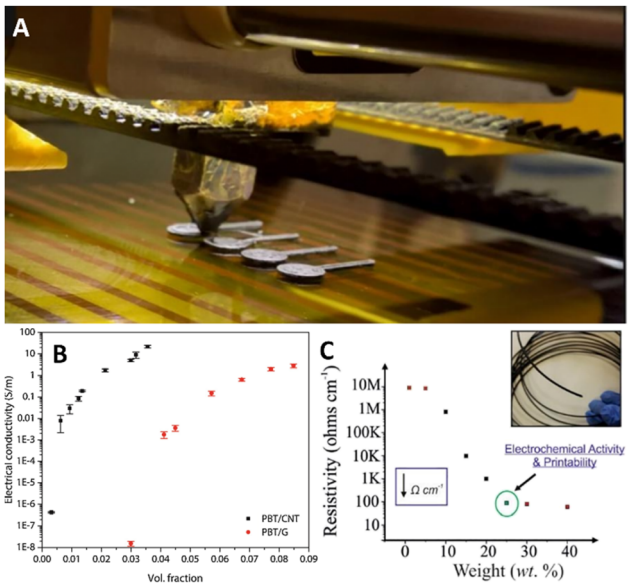

Fig. 6 (A) Fabrication of 25 wt% nanographite-loaded PLA electrode.[67] (B) Electrical conductivity plotted as a function of CNT and graphene volume fraction for 3D printed polymer nanocomposites.[66] (C) Resistivity *vs.* nanographite content.[67] Copyright, Elsevier B.V.

while maintaining suitable mechanical properties for printing applications[67] (Fig. 6A). The integration process typically involves melt extrusion mixing of the polymer with the conductive filler under carefully controlled temperature and shear conditions to achieve uniform dispersion without degrading the materials' properties.[69]

The optimization of these composites requires careful consideration of multiple interdependent parameters that significantly impact both printability and electrochemical performance. The percolation threshold represents a critical design parameter, marking the minimum filler concentration necessary to establish continuous conductive networks throughout the polymer matrix.[66,67] Research has shown that different fillers exhibit varying percolation thresholds – for example, carbon nanotubes achieve percolation at relatively low concentrations (0.31% v/v) compared to graphene (3.30% v/v) in polybutylene terephthalate matrices[66] (Fig. 6B). Beyond the percolation threshold, increasing filler content generally enhances conductivity but can adversely affect printing characteristics. This has been demonstrated in studies where excessive filler loading (>25 wt% for nanographite/PLA) led to brittle behavior and poor print quality[67] (Fig. 6C). Surface treatment and modification strategies have emerged as effective approaches to optimize the filler–matrix interface and enhance both electrical and mechanical properties. For instance, chemical functionalization of carbon nanotubes or graphene sheets can improve their dispersion within the polymer matrix and strengthen interfacial bonding.[70] The processing conditions during composite fabrication, including mixing temperature, shear rate, and cooling profiles, must be carefully controlled to prevent filler agglomeration and ensure uniform distribution throughout the matrix.[69,71] These parameters directly influence the final composite's performance in terms of conductivity, mechanical strength, and printing behavior.

Although PLA is classified as a biodegradable polymer, it generally degrades only under high-temperature composting conditions. In standard laboratory and field settings, PLA-based electrodes typically maintain mechanical integrity and electrochemical performance over routine testing periods. Nonetheless, prolonged exposure to moisture or certain chemicals can gradually weaken the polymer matrix, impacting electrode stability. This partial biodegradability could become advantageous in scenarios demanding reduced plastic waste, but care must be taken to characterize any performance loss over extended deployment times.

Carbon-based materials

Carbon-based materials have established themselves as the primary conductive fillers in fabricating 3D-printed electrochemical sensors, offering a unique combination of electrical conductivity, chemical stability, and versatile morphologies.[47,72] CB has emerged as the most widely adopted carbon filler, providing an optimal balance of conductivity and cost-effectiveness for practical applications.[73,74] The inherently small particle size of CB, typically ranging from 20–50 nm, coupled with its structured nature, enables the formation of extensive conductive networks within polymer matrices at relatively low loading levels, often between 15–25 wt%. This characteristic is particularly advantageous in FDM applications, where studies have shown that CB-based composites can achieve electrical conductivity values suitable for electrochemical sensing while maintaining printability.[32] For instance, Vanečková *et al.*[75] demonstrated that PLA/CB 3D-printed electrodes (Fig. 7A) exhibited comparable electrochemical behavior to conventional metallic and carbon electrodes, with anodic and cathodic potential peak separation values between 80–85 mV, indicating efficient electron transfer characteristics.

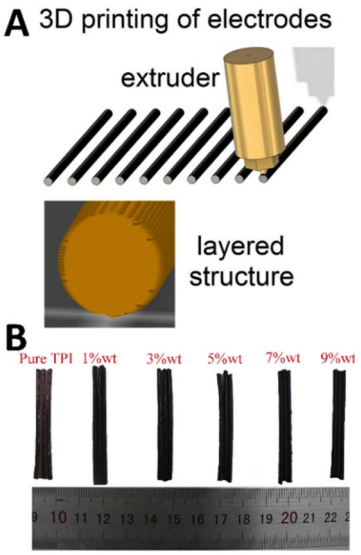

Fig. 7 (A) Geometry of PLA/CB 3D-printed electrodes. (B) Samples of pure TPI and CNTs-TPI$_{1,\ 3,\ 5,\ 7,\ 9wt\%}$ bars.[76] Copyright, Elsevier B.V.

Similarly, Rocha *et al.*[40] reported that activated PLA/CB 3D-printed electrodes showed exceptional sensitivity in detecting metal ions, achieving detection limits of 2.9 μg L^{-1} and 2.6 μg L^{-1} for Cd^{2+} and Pb^{2+} respectively, demonstrating the practical utility of CB-based composites in electrochemical sensing applications.

The integration of graphene and its derivatives as advanced carbon fillers has revolutionized the development of 3D-printed electrochemical sensors, primarily due to their extraordinary electrical properties and high surface area characteristics.[77] Recent studies have shown that incorporating graphene into thermoplastic matrices can enhance both electrical conductivity and mechanical properties significantly. For example, Gusmão *et al.*[33] conducted comprehensive research on PLA/graphene composites, demonstrating that solvent-activated electrodes significantly improved electrochemical performance, particularly when treated with polar aprotic solvents like DMF and acetone. Their findings showed enhanced electroactive surface areas and superior areal capacitance compared to conventional electrodes. However, researchers face persistent challenges in achieving uniform dispersion and preventing reagglomeration during the printing process, which can affect sensor performance.[66] CNTs, both in their single-walled and multi-walled forms, represent another promising category of carbon fillers, offering unique advantages in enhancing composite conductivity.[78] Wu and colleagues[76] investigated the development of thermoplastic polyimide (TPI) filaments with different CNT contents (1–9 wt%, Fig. 7B), identifying a percolation threshold at 3 wt% CNTs where optimal electrical properties were achieved. The study demonstrated that CNTs could effectively accommodate nucleation sites to bind with the reinforcing polymer matrix, though their widespread adoption remains limited by factors such as high production costs and processing complexities.[66]

Metal-containing filaments

Metal-containing filaments represent an emerging class of materials for 3D-printed electrochemical sensors, offering potential advantages in terms of conductivity and electrochemical activity (Fig. 8). These materials can be categorized into two main types: metal–polymer composites and metallic filaments. Metal–polymer composites typically incorporate metal particles or powders within a thermoplastic matrix, similar to carbon-based composites but offering unique electrochemical properties based on the specific metal used. Recent advances in this area include the incorporation of AuNPs into graphite–PLA composites through an eco-friendly synthesis approach, which demonstrated enhanced electrochemical performance with improved heterogeneous electron transfer rates and real electrochemical surface area for sensing applications.[79] Similarly, the integration of silver nanoparticles with graphite into PLA matrices has enabled the development of robust electrochemical sensors with improved charge transfer capabilities and excellent sensitivity towards analytes like pyridoxine.[80] Pure metallic filaments, while less common, provide exceptional electrical conductivity and electrochemical performance. For instance, fully metallic copper electrodes produced through fused filament

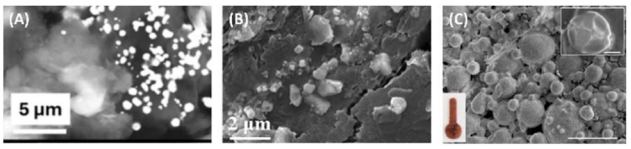

Fig. 8 SEM images of 3D printing material using (A) Au,[79] (B) Ag[80] and (C) Cu as filament.[81] Copyright, Elsevier B.V.

fabrication followed by sintering have shown promising results for non-enzymatic glucose sensing, demonstrating how the transition from composite to pure metal formulations can enhance sensing capabilities.[81] These materials often require specialized printing equipment capable of handling higher processing temperatures and more demanding printing conditions, as evidenced by the need for precise temperature control during sintering processes to maintain electrode shape and performance characteristics. The incorporation of metals such as copper, silver, and gold into printable formulations has enabled the development of sensors with enhanced sensitivity and selectivity for specific analytical applications, with recent examples showing detection limits in the parts per billion range for environmental contaminants.[79] These advances highlight the growing potential of metal-containing filaments in creating high-performance electrochemical sensing platforms through additive manufacturing approaches.

Novel material developments

Recent advances in material science have led to the development of innovative composites that expand the capabilities of 3D-printed electrochemical sensors. Metal–organic frameworks (MOFs) have been successfully incorporated into printable formulations, offering unique properties for selective chemical sensing. These materials combine high surface area and tailored pore structures with specific chemical functionality, enabling enhanced sensitivity and selectivity in environmental monitoring applications. In particular, several research groups have demonstrated the integration of MOFs with conductive carbon materials to create printable composites with superior electrochemical performance. For instance, calcium-based MOFs modified with carbon paste have shown exceptional sorption capabilities and electrochemical response for heavy metal detection, achieving detection limits in the sub-ppb range.[82] The versatility of MOFs is further exemplified by the development of iron-based MOF-MXene nanocomposites, where the synergistic combination of MOF's high surface area and MXene's electrical conductivity enables rapid electron transfer and enhanced electrocatalytic activity.[83] These hybrid materials can be effectively incorporated into 3D-printable inks while maintaining their functional properties. Beyond material development, researchers have also made significant progress in optimizing printing parameters and electrode architectures. The emergence of dual-extruder 3D printing technology has enabled the fabrication of integrated electrochemical cells with both conductive and non-conductive components in a single step.[84] This approach not only simplifies the manufacturing process but also ensures better reproducibility and stability of

the printed sensors. The combination of MOFs with 3D printing has particularly shown promise in environmental monitoring applications, such as heavy metal detection in water samples and glucose sensing in biological fluids.[85] Recent studies have demonstrated that 3D-printed MOF-based electrodes can maintain their analytical performance over extended periods while offering the advantages of easy surface renewal and low-cost fabrication. These developments represent a significant step forward in making advanced electrochemical sensors more accessible for routine environmental monitoring applications.

3D printing followed by pyrolysis for carbon electrodes

3D printing followed by pyrolysis offers a powerful approach for fabricating high-performance carbon electrodes. In this process, polymer-based 3D-printed structures—often containing carbon additives—are subjected to controlled high-temperature treatments under inert atmospheres to remove the polymer binder and convert remaining carbon precursors into a conductive, carbon-rich framework.[86,87] This technique capitalizes on the design freedom of additive manufacturing while producing pyrolytic carbon electrodes with enhanced mechanical stability, large electroactive surface areas, and robust chemical resistance.[88]

Recent studies have demonstrated that pyrolyzed 3D-printed carbon electrodes can achieve excellent electron transfer characteristics and facilitate sensitive detection of diverse analytes, including biomolecules and environmental contaminants.[89,90] Notably, the micro- and nano-scaled porosity introduced during pyrolysis promotes efficient mass transport, which is essential for high sensitivity. For instance, researchers have printed polymeric scaffolds with deliberate pore structures that, upon pyrolysis, yield intricate conductive networks suitable for electrochemical sensing.[87] The resulting electrodes are versatile and have shown promise for *in vivo* neurochemical measurements, pesticide screening, and heavy metal analysis.

Despite these advantages, challenges remain. The shrinkage and deformation that occur during high-temperature treatment must be carefully managed through precise thermal profiles and resin formulations.[87] Achieving reproducible electrode geometries with minimal warping requires optimization of both 3D printing conditions (*e.g.*, nozzle size, infill density) and pyrolysis parameters (*e.g.*, heating rate, dwell time). Another limitation is the need for specialized equipment capable of reaching temperatures above 800 °C under inert environments. Nevertheless, the resultant pyrolyzed carbon often exhibits superior electrochemical performance compared to unpyrolyzed conductive composites, making this technique a compelling choice for advanced applications.[86,91]

Ongoing research aims to refine pyrolysis protocols and resin chemistries to further improve the structural fidelity and electrical conductivity of 3D-printed carbon electrodes. Additionally, integrating functional nanomaterials or metal catalysts before pyrolysis has shown potential for enhancing sensitivity and selectivity. As these methods evolve, 3D-printed pyrolyzed carbon electrodes are poised to play an increasingly important role in electrochemical sensing, offering customizable designs and excellent performance for environmental, biological, and industrial monitoring applications.

Lab-made *vs.* commercial filaments

Table 2 below summarizes key materials commonly employed in 3D-printed electrochemical sensing devices and highlights their compatible printing technologies, along with the primary advantages, limitations, and representative electrochemical performances reported in the literature. This overview illustrates how specific materials are more suitable for certain printing approaches and demonstrates how selecting the optimal material–printing process combination can profoundly influence sensor conductivity, mechanical integrity, and overall analytical performance. The choice between commercial and laboratory-made filaments presents important considerations for sensor development. Commercial filaments offer convenience and consistency but often come with limitations in terms of conductivity and material composition. These materials typically contain 10–20% conductive filler by weight and are optimized for printing reliability rather than electrochemical performance.[92]

Laboratory-made filaments provide greater flexibility in material composition and properties but require careful optimization of processing conditions. These custom formulations can incorporate higher filler loadings, novel material combinations, and specific functional additives tailored to particular sensing applications. The production process typically involves mixing the conductive filler with the polymer matrix in the presence of solvents, followed by extrusion to create filaments of controlled diameter.[93] The development of lab-made filaments has demonstrated the potential for achieving higher conductivity than commercial alternatives, with some formulations showing conductivity improvements of several orders of magnitude.[94] However, these materials often face challenges in terms of mechanical properties and printing reliability. The trade-off between enhanced electrical properties and practical printability remains a key consideration in the development of new filament formulations.

Furthermore, the cost implications of commercial *versus* lab-made filaments must be considered. While commercial filaments are more expensive per unit weight than their raw materials, the investment in equipment and time required for laboratory production can make custom filament development economically viable only for specialized applications or research purposes.[13,25,29] The choice between commercial and lab-made filaments ultimately depends on the specific requirements of the intended application, including performance needs, production volume, and available resources.

Surface modification and optimization strategies

Electrochemical and chemical activation

Electrochemical activation represents a fundamental approach to enhancing the performance of 3D-printed electrodes. This process typically involves applying controlled potential or

Table 2 Summary of 3D printing technologies and material compositions used for electrochemical sensors

Material composition	Compatible 3D printing technology	Strengths	Limitations
Carbon-based composites	FDM	- Cost-effective, widely available filaments - Straightforward post-processing - Tunable conductivity *via* filler loading	- Lower electrical conductivity compared to metals - Surface roughness often requires polishing/chemical activation - Possible filler agglomeration if not well dispersed
Metal–polymer composites	FDM	- Enhanced conductivity relative to purely carbon-based filaments - Potential for enzyme-free catalytic activity	- Often more expensive - Filler homogeneity can be challenging - Limited commercial availability
Metal resins/powders	SLM; binder jetting	- High electrical conductivity - Excellent mechanical robustness - Complex geometries feasible	- Specialized, expensive printers - Handling metallic powders requires safety precautions - Thermal stress may cause warping
Photopolymer resins with conductive fillers	SLA	- High-resolution prints - Smooth surface finish - Customizable geometry for microfluidics	- Fewer conductive photopolymer resins available - Post-curing steps often needed - Potentially lower mechanical strength *vs.* SLM
Polymer precursors for pyrolyzed carbon	DIW; FDM followed by pyrolysis	- Produces highly conductive, porous carbon - Large electroactive surface area - Exceptional chemical stability	- Requires high-temperature pyrolysis - Possible shrinkage and shape deformation - Specialized thermal equipment needed

current signals to modify the electrode surface, creating functional groups and increasing the active surface area. Recent studies have demonstrated that electrochemical activation can be performed through various methods, including potentiodynamic cycling, constant potential application, or controlled current processes in suitable electrolyte solutions. For carbon black-doped poly(lactic acid) (PLA-CB) electrodes, electrochemical pretreatment through oxidation at 1.8 V followed by reduction at −1.8 V effectively removes the insulating polymer layer and exposes the carbon black particles.[95] This activation process has been shown to enhance electron transfer kinetics and improve the electrochemical response. The exposed carbon sites provide more active areas for analyte interaction and detection. Chemical treatment methods offer another powerful strategy for modifying 3D-printed electrode surfaces. These approaches typically involve exposing the electrode to specific chemical reagents that can selectively remove the polymer matrix, expose conductive materials, or introduce functional groups. For example, Silva-Neto *et al.*[96] achieved significant improvements in electrode performance by combining electrochemical oxidation with Fenton processes, applying 1.8 V for 200 s in 6 M acetic acid as supporting electrolyte (Fig. 9A). This combined approach led to remarkable increases in peak currents of up to 353% and enhanced heterogeneous rate constants. In addition, studies have shown that chemical activation using DMF or NaOH removes the PLA matrix more efficiently compared to acid treatments.[98] The combination of chemical treatment with electrochemical activation can lead to synergistic effects, resulting in higher structural defects (increased ID/IG ratio in Raman spectroscopy) and improved heterogeneous electron transfer.

During activation, the applied potential or current can induce oxidation or reduction of the electrode material, leading to the formation of oxygen-containing functional groups such as carboxyl, hydroxyl, and carbonyl moieties. Browne *et al.*[97] demonstrated that electrochemical activation combined with DMF treatment could dramatically improve electron transfer rates (Fig. 9B), with heterogeneous electron transfer rate constants reaching 1.2×10^{-3} cm s^{-1}. These surface functionalities enhance the electrode's wettability and provide active sites for electron transfer processes. Additionally, the activation

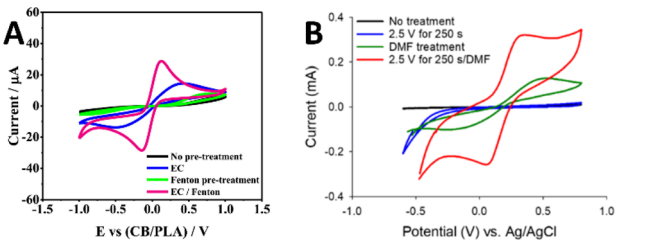

Fig. 9 (A) CVs recorded in the presence of $[Fe(CN)_6]^{4-/3-}$ using 3D printed electrodes with no pre-treatment, treated *via* electrochemical approach, Fenton process and both electrochemical/Fenton activation.[96] (B) CVs recorded in the presence of $[Fe(CN)_6]^{4-/3-}$ using DMF-treated 3D electrodes.[97] Copyright, Elsevier B.V. and American Chemical Society.

process can expose previously buried conductive materials within the polymer matrix, effectively increasing the electroactive surface area. This was evidenced by Silva-Neto *et al.*'s[96] work showing significant reductions in charge transfer resistance from several thousand ohms to 1376 ± 10 Ω after activation.

The optimization of activation parameters, including potential range, scan rate, and treatment duration, plays a crucial role in achieving desired surface properties. Recent work by Hernández-Rodríguez *et al.*[99] demonstrated that spark discharge activation could serve as a rapid and green alternative, completing the process in just 30 seconds while achieving comparable improvements in electron transfer kinetics. Their approach highlighted how excessive activation can lead to surface degradation or loss of mechanical stability, while insufficient treatment may not provide adequate enhancement of electrochemical performance. The choice of electrolyte solution also influences the activation process, with different media promoting various types of surface modifications. For instance, Silva-Neto *et al.*[96] found that using acetic acid as supporting electrolyte during electrochemical activation helped maintain long-term stability by providing another source of organic compounds to be degraded by excess hydroxide radicals. This careful optimization of activation parameters has enabled the development of 3D-printed electrodes with enhanced sensitivity and stability for various electroanalytical applications.

Surface modification with conducting polymers represents an innovative strategy to enhance the electrochemical properties of 3D-printed electrodes. For instance, poly(methylene blue) (PMB) has been successfully electrodeposited on PLA-CB electrodes using various electrochemical techniques like cyclic voltammetry, chronopotentiometry, and chronoamperometry.[100] The electropolymerization process creates a thin conductive polymer layer that exhibits fast electron transfer properties. XPS analysis has confirmed the formation of PMB doped with counter ions on the electrode surface, while EIS measurements have shown significantly reduced charge transfer resistance after polymer modification. The surface morphology also undergoes notable changes after modification. SEM analysis reveals that polymer coating can lead to more homogeneous and uniform surfaces. In the case of PMB modification, the electrode surface transitions from an inhomogeneous distribution of aggregated particles to a more even morphology with visible microspherical grains structured in random stacks. More recently, poly(3,4-ethylenedioxythiophene):poly(styrene sulfonate) (PEDOT:PSS) has emerged as a promising conductive polymer for electrode modification due to its excellent film-forming properties, environmental friendliness, and direct electron transfer capabilities.[101] Liao *et al.*[102] reported that PEDOT:PSS modification decreased the electron transfer resistance from 262.4 Ω to 173.5 Ω (Fig. 10A), indicating substantially improved conductivity. When PEDOT:PSS composites are applied to gold nanoparticle-modified 3D printed electrodes (SACP@Au@3DE), SEM imaging shows the formation of a uniform conductive film covering the electrode surface (Fig. 10B). These polymer

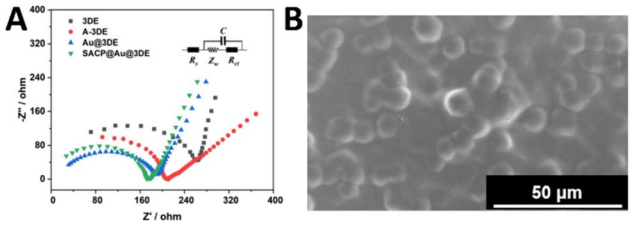

Fig. 10 (A) EIS of 3DE, A-3DE, Au@3DE and SACP@Au@3DE with frequencies between 1 and 1 × 10^6 Hz. (B) SEM of prepared SACP@Au@3DE.[102] Copyright, Elsevier B.V.

modifications not only improve conductivity but also expand the potential applications of 3D-printed electrodes in various sensing applications, such as the detection of bioactive compounds like chlorogenic acid with enhanced sensitivity and wider linear detection ranges compared to unmodified electrodes.

Nanomaterial incorporation

The incorporation of nanomaterials represents an advanced strategy for enhancing the performance of 3D-printed electrochemical sensors. This approach can be implemented either during the electrode fabrication process or as a post-printing modification. Recent studies have demonstrated remarkable success with various nanomaterials such as metal nanoparticles, carbon nanotubes, and graphene derivatives that significantly improve conductivity, catalytic activity, and sensing capabilities. For instance, silver nanoparticles (AgNPs) fabricated through green synthesis methods and incorporated into 3D-printed electrodes have shown excellent sensitivity for H_2O_2 detection, achieving detection limits as low as 0.52 μM with impressive linear range capabilities.[103]

Surface modification with nanomaterials can be achieved through various methods, including electrodeposition, drop-casting, and *in situ* synthesis. A notable example is the fabrication of nanoscale-thick silver thin films (Ag-NTF) on substrates using electrochemical 3D printing (Fig. 11), which demonstrated enhanced electrochemical activity and achieved a sensitivity of 25 ± 1 μA mM^{-1} cm^{-2} for H_2O_2 sensing.[104] The selection of appropriate nanomaterials and modification techniques depends on the specific requirements of the intended analytical application, including target analyte characteristics

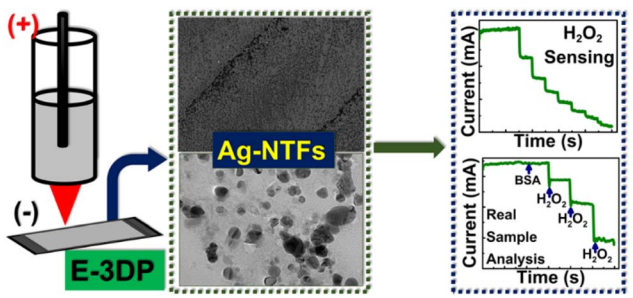

Fig. 11 Fabrication of Ag-NTF on substrates using electrochemical 3D printing for H_2O_2 detection.[104] Copyright, American Chemical Society.

and desired performance metrics. The synergistic effects between different nanomaterials can be exploited to create composite modifications with enhanced functionality. For instance, combining graphene-doped PLA (G-PLA) with AgNPs has shown remarkable improvements in electron transfer kinetics and sensing capabilities.[105] Studies have demonstrated that such composite materials can achieve detection limits in the micromolar range while maintaining excellent selectivity and stability. The careful control of nanomaterial size, distribution, and surface coverage is essential for optimizing sensor performance, as evidenced by research showing that AgNPs with average particle sizes of 21 nm exhibited optimal electrochemical activity when uniformly distributed across the electrode surface. Through careful optimization of printing parameters and nanomaterial incorporation strategies, researchers have achieved significant improvements in sensor performance metrics. This includes enhanced sensitivity, lower detection limits, and improved stability compared to conventional electrode materials. The integration of nanomaterials through 3D printing processes has also addressed common challenges in sensor fabrication, such as reproducibility and scalability, while maintaining the advantages of customizable design and rapid prototyping capabilities inherent to additive manufacturing approaches.

3D-printed electrochemical sensor for environmental analytes sensing

Pathogen

The detection of pathogens using 3D-printed electrochemical sensors has shown promising results for rapid on-site analysis. These sensors enable the detection of various microorganisms, including bacteria and viruses, with high sensitivity and specificity. For instance, researchers have developed 3D-printed flexible devices that combine sampling and detection capabilities, allowing for efficient pathogen monitoring in environmental samples.[106] A notable example is the development of a 3D-printed electrochemical sensor for detecting *Listeria monocytogenes*, a significant foodborne pathogen. Rivas-Macho *et al.*[107] designed a sensor that combines loop-mediated isothermal amplification (LAMP) with electrochemical detection in a 3D-printed microfluidic chip. The sensor achieved impressive detection limits of 1.25 pg DNA per reaction and demonstrated specificity for all 12 L. monocytogenes serotypes. What makes this sensor particularly innovative is its ability to detect as little as 1 CFU/25 g in food samples. Another significant advancement comes from Martins *et al.*,[108] who developed a 3D-printed electrode platform for virus detection, specifically focusing on Hantavirus (Fig. 12A). Their sensor utilized a commercial 3D conductive filament of carbon black and PLA, with the unique feature of having naturally present carboxylic groups that enabled direct biomolecule anchoring without additional pretreatment. This sensor demonstrated a detection range of 30–240 μg mL^{-1} with a limit of detection of 22 μg mL^{-1}, showing promise for viral disease diagnosis. Stefano *et al.*[37] took a different approach by developing a new conductive filament

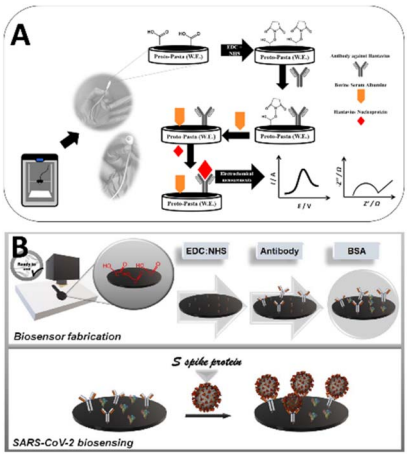

Fig. 12 Fabrication of 3D-printed electrochemical immunosensors for (A) *Listeria monocytogenes*[107] and (B) SARS-CoV-2 detection.[37] Copyright, Elsevier B.V.

ready-to-use for 3D-printing electrochemical biosensors. Their work focused on SARS-CoV-2 detection, demonstrating how 3D printing technology can be rapidly adapted for emerging infectious diseases. The sensor showed a linear range from 5.0 to 75.0 nM with a detection limit of 1.36 nM, making it suitable for clinical applications. As shown in Fig. 12B, their sensor design incorporated gold electrodes and a microfluidic chamber, enabling efficient sample handling and detection.

The integration of different materials and detection strategies has particularly advanced the field. The use of conductive filaments containing carbon-based materials in PLA matrices has become increasingly common, offering good electrical conductivity while maintaining printability. Many sensors incorporate additional functionalities such as microfluidic channels for sample handling or surface modifications for improved sensitivity and selectivity.[109,110] The success of these sensors in detecting various pathogens demonstrates their versatility and potential for broader applications in environmental monitoring, food safety, and clinical diagnostics.

Antibiotics

The monitoring of antibiotic residues in environmental samples has become increasingly important due to growing concerns about antimicrobial resistance. 3D-printed electrochemical sensors offer a practical solution for detecting various antibiotics in water and soil samples. These sensors typically incorporate selective recognition elements onto 3D-printed electrode surfaces, providing enhanced sensitivity through their three-dimensional architecture compared to conventional planar electrodes. For example, Lisboa *et al.*[93] developed a 3D-printed electrode using graphite/PLA composite filaments for sulfanilamide detection in environmental samples. Their sensor achieved excellent analytical performance with a detection limit of 12 nM and showed good selectivity towards other antibiotic classes. The sensor design incorporated a simple surface treatment protocol that enhanced its electrochemical response while maintaining cost-effectiveness.

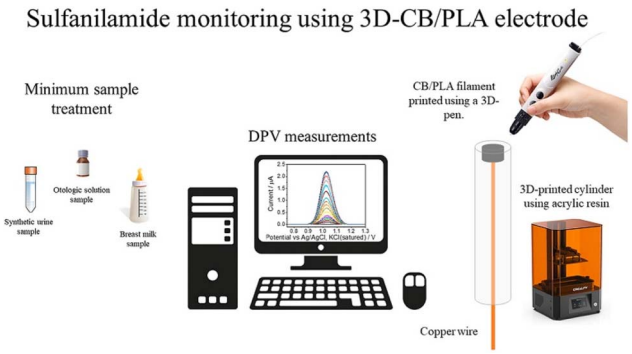

Fig. 13 3D-printed electrode for sulfanilamide monitoring.[112] Copyright, Elsevier B.V.

Another innovative approach was demonstrated by Lopes *et al.*,[111] who created a 3D-printed electrode using graphite dispersed in PLA matrix for tetracycline determination. Their sensor exhibited favorable charge transfer characteristics and could detect tetracycline in the submicromolar concentration range. The electrode's unique surface morphology showed non-uniformly distributed graphite sheets resulting in a highly porous surface that enhanced analyte interaction. Further advancing this field, Lisboa *et al.*[112] developed a cost-effective protocol using a 3D pen and lab-made filaments for ciprofloxacin sensing. As shown in Fig. 13, the electrode fabrication process involved a simple layer-by-layer deposition technique that produced reliable and reproducible sensors. Their method achieved a detection limit of 1.79 μM with excellent selectivity against common interfering compounds.

The incorporation of nanomaterials has also proven beneficial in enhancing sensor performance. Domingo-Roca *et al.*[113] demonstrated a fully 3D-printed impedance-based biosensor for rapid assessment of antibiotic susceptibility. Their sensor utilized gel modification and silver nanoparticles to improve sensitivity, allowing for antibiotic susceptibility testing within 90 minutes – significantly faster than conventional methods requiring 24–48 hours. The advantages of 3D-printed electrochemical sensors over traditional detection methods are significant. Their cost-effectiveness stems from using readily available materials like PLA and graphite, combined with simple fabrication processes, making them economically viable for widespread deployment. The customizability offered by 3D-printing technology enables rapid prototyping and optimization of electrode designs to suit specific detection requirements. The three-dimensional architecture and possibility of surface modification provide improved analyte interaction and detection capabilities, while enabling rapid analysis suitable for on-site environmental monitoring. Many of these sensors can analyze samples with simple dilution steps, reducing the complexity of analysis.[114]

Organophosphates

The detection of organophosphate pesticides using 3D-printed electrochemical sensors has gained significant attention due to their severe environmental and health impacts. These compounds, widely used as pesticides and chemical warfare agents, pose substantial risks to the biosphere, particularly when disposed of improperly in oceans and water bodies. Recent developments in 3D printing technology have revolutionized sensor fabrication, offering advantages such as rapid prototyping, customizable geometries, and cost-effectiveness in electrode production. A recent example in this field involves the development of 3D-printed nanocarbon electrodes (3DnCEs) using FDM. As demonstrated by Jyoti *et al.*,[115] these electrodes can be fabricated using conductive nanocarbon/PLA filaments and activated through DMF treatment, resulting in enhanced electrical conductivity and sensing capabilities. The surface morphology changes before and after DMF activation, showing the exposure of nanocarbon filaments that significantly improves electrochemical performance. The activated 3DnCEs demonstrated remarkable sensitivity towards various organophosphates, including methyl parathion, paraoxon, and fenitrothion, with detection limits reaching 0.5 μM. Another innovative approach, presented by Wei *et al.*,[116] integrates three-dimensional cell-based electrochemical biosensors with screen-printed carbon electrodes modified with zeolite imidazolate framework-67@CoAl layered double hydroxides/multi-walled carbon nanotube composites. This system achieved impressive detection limits of 0.148 μM for organophosphate compounds, utilizing acetylcholinesterase (AChE) as a bio-recognition element. The integration of 3D cell culture within the sensing platform provides an *in vivo*-like environment, enhancing the reliability of toxicological evaluations. The durability and reusability of these 3D-printed sensors make them particularly suitable for field-based pesticide monitoring. Studies have shown that these sensors maintain up to 93.2% of their initial response after four weeks of storage, demonstrating excellent stability. The electrochemical detection mechanism typically involves either direct reduction of organophosphates or indirect measurement through enzyme inhibition, allowing for rapid and sensitive analysis without complex sample preparation.

Heavy metal ions

The printing technology allows for the fabrication of complex electrode structures that can incorporate metal-specific recognition elements or modified surfaces for selective metal ion detection. Recent advances in materials and fabrication methods have enabled significant improvements in sensor performance and reliability. For example, Santangelo *et al.*[117] demonstrated an epitaxial graphene sensor combined with 3D-printed microfluidic chips that achieved detection limits of 95 nM for lead ions, with good stability and reproducibility over time. Their system showed particular promise due to its real-time monitoring capabilities and reusable lab-on-chip design. Similarly, Walters *et al.*[42] developed graphene/PLA composite electrodes capable of detecting mercury at concentrations as low as 6.1 nM, while also showing sensitivity to lead and cadmium when modified with bismuth microparticles.

The choice of electrode materials and surface modifications plays a crucial role in sensor performance. Shin *et al.*[118] showed

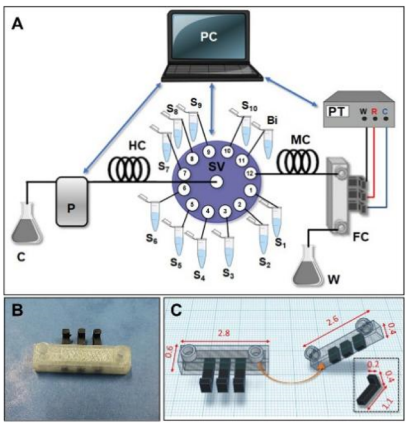

Fig. 14 (A) Schematic illustration of the sequential injection/anodic stripping system. (B) Photograph of the microfluidic device. (C) The dimensions of the microfluidic device, the fluidic channel and the integrated electrodes.[119] Copyright, Elsevier B.V.

that acid pretreatment of 3D-printed PLA/graphite/graphene oxide (PLA/Gr/GO) electrodes significantly enhanced their sensitivity, achieving detection limits of 0.039–0.13 ppb for various heavy metals. This improvement was attributed to better exposure of active sites and enhanced electron transfer properties. The integration of nanomaterials, particularly graphene-based materials, has become increasingly common due to their excellent electrical properties and high surface area.

Another innovative approach was demonstrated by Baltima *et al.*,[119] who developed a 3D-printed fluidic electrochemical microcell for sequential injection/stripping analysis (Fig. 14). Their system achieved detection limits of 0.38 μg L^{-1} for lead and 0.57 μg L^{-1} for cadmium, with excellent reproducibility (RSD < 4.5%). The integration of microfluidic components with 3D-printed electrodes enables automated sample handling and improved analytical performance.

The practical applications of these sensors extend beyond laboratory settings. Multiple studies have validated their performance using real environmental samples, including drinking water, wastewater, and certified reference materials. For instance, Shin *et al.*[118] successfully analyzed European Reference Materials for heavy metals using their pretreated PLA/Gr/GO electrode, demonstrating excellent agreement with conventional analytical methods. This validates the potential of 3D-printed sensors for real-world environmental monitoring applications (Table 3).

Current challenges and future perspectives

Technical limitations

The development and implementation of 3D-printed electrochemical sensors face several significant technical challenges that continue to influence their widespread adoption in environmental monitoring applications. One fundamental

Table 3 Summary of selected 3D-printed electrochemical sensors for environmental analytes

Target analyte	Electrode design	Electrochemical method	Analytical performance	References
Pathogens (*Listeria monocytogenes*)	3D-printed microfluidic chip integrating LAMP with electrochemical detection	Voltammetric readout	LOD: 1.25 pg DNA; 1 CFU/25 g in food samples	107
Pathogens (Hantavirus)	3D-printed conductive CB/PLA electrode for viral antigen detection	Immunosensor with amperometric or voltammetric transduction	LOD: 22 μg mL^{-1} for Hantavirus	108
Pathogens (SARS-CoV-2)	3D-printed, ready-to-use conductive filament (custom CB/PLA) electrode for SARS-CoV-2	Voltammetric detection	LOD: 1.36 nM	37
Antibiotics (Sulfanilamide)	3D-printed graphite/PLA electrode for sulfanilamide	Differential pulse voltammetry (DPV)	LOD: 12 nM	93
Antibiotics (Tetracycline)	3D-printed graphite/PLA electrode with microfluidic platform for tetracycline	Square-wave voltammetry	Submicromolar detection range	111
Antibiotics (Ciprofloxacin)	3D-printed layer-by-layer graphite/PLA electrode using a 3D pen for ciprofloxacin	DPV	LOD: 1.79 μM	112
Organophosphates (methyl parathion, paraoxon,*etc.*)	3D-printed nanocarbon/PLA electrode (activated with DMF)	Voltammetric detection	LOD: ~0.5 μM for methyl parathion, paraoxon, fenitrothion	115
Heavy metals	3D-printed graphene/PLA composite electrode	Anodic stripping voltammetry	LOD: 6.1 nM (Hg^{2+}); also sensitive to Pb^{2+} and Cd^{2+}	42
Heavy metals	Pretreated (acid-activated) PLA/graphite/graphene oxide electrode	Anodic stripping voltammetry	LOD: 0.039–0.13 ppb (various heavy metals)	118
Heavy metals	3D-printed microfluidic device with integrated electrodes	Sequential injection/stripping analysis	LOD: 0.38 μg L^{-1} (Pb^{2+}), 0.57 μg L^{-1} (Cd^{2+})	119

limitation lies in the achievable resolution and precision of current printing technologies, particularly when using conductive composite materials. While FDM printing represents the most accessible approach, its resolution constraints can affect the reproducibility and consistency of electrode surfaces, potentially impacting analytical performance. The layer-by-layer nature of the printing process introduces inherent structural heterogeneities that can affect electron transfer kinetics and overall sensor performance. These irregularities become particularly problematic when developing sensors for trace analysis, where surface uniformity plays a crucial role in achieving high sensitivity and reproducibility. Additionally, the thermal processing required during printing can affect the distribution and connectivity of conductive materials within the polymer matrix, leading to variations in electrical conductivity across different printed batches. Another significant technical challenge involves the integration of multiple materials and functionalities within a single printed device. While dual-extrusion systems enable the combination of conductive and non-conductive materials, achieving precise control over interface properties and ensuring robust electrical connections remains challenging. The development of more sophisticated printing approaches that can handle multiple materials with different physical properties will be essential for advancing sensor capabilities. Beyond biodegradable PLA, other 3D-printed electrodes include metal–polymer composites or pyrolyzed carbon, whose end-of-life pathways can be less straightforward. Metal-containing prints can leach ions if disposed of improperly, whereas carbon electrodes may persist in the environment. However, many metallic or carbon-based parts can be reclaimed through recycling or thermal treatments. Developments in recyclable polymers and the establishment of standardized recycling protocols for composite filaments could further mitigate environmental impact, thus enhancing the sustainability of 3D-printed sensors.

Material constraints

Current material limitations represent a significant bottleneck in the advancement of 3D-printed electrochemical sensors. The available commercial conductive filaments typically exhibit relatively low electrical conductivity compared to traditional electrode materials, necessitating various post-processing steps to achieve adequate electrochemical performance. The trade-off between conductivity and printability continues to challenge material developers, as increasing the conductive filler content often compromises the mechanical properties and printing characteristics of the composites. The long-term stability of printed materials presents another crucial consideration. Environmental exposure, mechanical stress, and repeated electrochemical cycling can lead to degradation of sensor performance over time. The development of more robust materials that maintain their electrical and mechanical properties under various operating conditions remains an important research priority. Additionally, the limited availability of specialized printing materials, particularly those incorporating novel functional components, restricts the exploration of advanced sensing capabilities. The cost of conductive printing materials also poses a significant constraint, particularly for large-scale applications. Commercial conductive filaments are substantially more expensive than traditional electrode materials, potentially limiting their adoption in routine environmental monitoring applications. The development of more cost-effective material formulations, possibly incorporating recycled or sustainable components, could help address this limitation.

Commercialization prospects

The commercialization potential of 3D-printed electrochemical sensors for environmental applications depends on several key factors. The ability to scale up production while maintaining consistent performance characteristics represents a primary consideration. Current manufacturing approaches often involve manual post-processing steps that could limit large-scale production efficiency. The development of automated manufacturing processes that integrate printing and surface modification steps could enhance commercial viability. Market acceptance will depend on demonstrating clear advantages over existing sensing technologies in terms of cost, performance, or functionality. While 3D-printed sensors offer benefits in terms of customization and rapid prototyping, they must compete with established sensor technologies in terms of reliability, sensitivity, and ease of use. The identification of specific application niches where the unique capabilities of 3D-printed sensors provide compelling advantages could drive initial commercial adoption. The regulatory landscape surrounding 3D-printed analytical devices also influences commercialization prospects. Establishing appropriate quality control measures and obtaining necessary certifications for environmental monitoring applications will be crucial for market entry. Additionally, intellectual property considerations surrounding both printing technologies and material formulations may affect commercialization strategies.

Research opportunities

The field of 3D-printed electrochemical sensors presents numerous opportunities for innovative research and development. Advanced material design represents a particularly promising area, including the development of new composite formulations that optimize both printability and electrochemical performance. The exploration of novel conductive fillers, smart materials, and biomimetic components could lead to sensors with enhanced sensitivity and selectivity. The integration of artificial intelligence and machine learning approaches offers opportunities for optimizing printing parameters and predicting sensor performance based on design characteristics. These computational tools could accelerate the development process and enable more efficient exploration of the vast design space available through 3D printing. Additionally, the development of *in situ* monitoring techniques for assessing printing quality and electrode performance could improve manufacturing reliability. Research into novel sensing mechanisms and detection strategies specifically suited to 3D-

printed platforms could expand the capabilities of these devices. This includes the development of integrated sample preparation and analysis systems, multiplexed detection platforms, and sensors incorporating advanced recognition elements. The combination of 3D printing with other fabrication technologies might also enable new device architectures and functionalities not achievable through conventional methods.

Furthermore, the exploration of sustainable materials and manufacturing approaches represents an important research direction. This includes the development of biodegradable sensor materials, the incorporation of recycled components, and the optimization of resource-efficient manufacturing processes. Such developments could enhance the environmental sustainability of sensor production while potentially reducing costs.

Data availability

No primary research results, software or code have been included and no new data were generated or analysed as part of this review.

Author contributions

Shuduan Mao: conceptualization, supervision, methodology, writing – original draft, funding acquisition, project administration. Liangliang Pan: investigation, formal analysis, data curation, visualization. Shijing Zhou: investigation, formal analysis, data curation. Jiaying Yang: investigation, data curation. Tongyun Fei: investigation, data curation. Li Fu: supervision, writing – review & editing. Cheng-Te Lin: supervision, writing – review & editing.

Conflicts of interest

There are no conflicts to declare.

Acknowledgements

This work was funded by the National Natural Science Foundation of China (No. 42307512), the Natural Science Foundation of Zhejiang Province (No. LQ23D030001), and Zhejiang Shuren University Basic Scientific Research Special Funds.

References

1 G.-L. Yang, X.-L. Jiang, H. Xu and B. Zhao, *Small*, 2021, **17**, 2005327.
2 S. R. Benjamin and E. J. Miranda Ribeiro Júnior, *Curr. Opin. Environ. Sci. Health*, 2022, **29**, 100381.
3 A. Rhouati, M. Berkani, Y. Vasseghian and N. Golzadeh, *Chemosphere*, 2022, **291**, 132921.
4 A. Thakur and A. Kumar, *Sci. Total Environ.*, 2022, **834**, 155219.
5 A. Yusuf, A. Sodiq, A. Giwa, J. Eke, O. Pikuda, J. O. Eniola, B. Ajiwokewu, N. S. Sambudi and M. R. Bilad, *Environ. Pollut.*, 2022, **292**, 118421.
6 S. Tajik, H. Beitollahi, F. G. Nejad, Z. Dourandish, M. A. Khalilzadeh, H. W. Jang, R. A. Venditti, R. S. Varma and M. Shokouhimehr, *Ind. Eng. Chem. Res.*, 2021, **60**, 1112–1136.
7 H. Kumar, N. Kumari and R. Sharma, *Environ. Impact Assess. Rev.*, 2020, **85**, 106438.
8 S. Tajik, H. Beitollahi, F. G. Nejad, I. Sheikhshoaie, A. S. Nugraha, H. W. Jang, Y. Yamauchi and M. Shokouhimehr, *J. Mater. Chem. A*, 2021, **9**, 8195–8220.
9 A. Khanmohammadi, A. Jalili Ghazizadeh, P. Hashemi, A. Afkhami, F. Arduini and H. Bagheri, *J. Iran. Chem. Soc.*, 2020, **17**, 2429–2447.
10 Q. He, B. Wang, J. Liang, J. Liu, B. Liang, G. Li, Y. Long, G. Zhang and H. Liu, *Mater. Today Adv.*, 2023, **17**, 100340.
11 Y. Xu, X. Wu, X. Guo, B. Kong, M. Zhang, X. Qian, S. Mi and W. Sun, *Sensors*, 2017, **17**, 1166.
12 Y. Ni, R. Ji, K. Long, T. Bu, K. Chen and S. Zhuang, *Appl. Spectrosc. Rev.*, 2017, **52**(7), 623–652.
13 R. M. Cardoso, D. M. H. Mendonça, W. P. Silva, M. N. T. Silva, E. Nossol, R. A. B. da Silva, E. M. Richter and R. A. A. Muñoz, *Anal. Chim. Acta*, 2018, **1033**, 49–57.
14 M. P. Browne, E. Redondo and M. Pumera, *Chem. Rev.*, 2020, **120**, 2783–2810.
15 Y. Chang, Q. Cao and B. J. Venton, *Curr. Opin. Electrochem.*, 2023, **38**, 101228.
16 W. B. Veloso, T. R. L. C. Paixão and G. N. Meloni, *Electrochim. Acta*, 2023, **449**, 142166.
17 C. Y. Foo, H. N. Lim, M. A. Mahdi, M. H. Wahid and N. M. Huang, *Sci. Rep.*, 2018, **8**, 7399.
18 R. G. Rocha, D. L. O. Ramos, L. V. de Faria, R. L. Germscheidt, D. P. dos Santos, J. A. Bonacin, R. A. A. Munoz and E. M. Richter, *J. Electroanal. Chem.*, 2022, **925**, 116910.
19 M. A. B. Helú and L. Liu, *Electrochim. Acta*, 2021, **365**, 137279.
20 H. Yuk, B. Lu, S. Lin, K. Qu, J. Xu, J. Luo and X. Zhao, *Nat. Commun.*, 2020, **11**, 1604.
21 M. Deka, N. Sinha, R. Das, N. K. Hazarika, H. Das, B. Daurai and M. Gogoi, *Anal. Methods*, 2024, **16**, 485–495.
22 U. S. Jayapiriya and S. Goel, *Sustain. Energy Technol. Assess*, 2020, **42**, 100811.
23 A. Ambrosi and M. Pumera, *Chem. Soc. Rev.*, 2016, **45**, 2740–2755.
24 G. L. Goh, M. F. Tay, J. M. Lee, J. S. Ho, L. N. Sim, W. Y. Yeong and T. H. Chong, *Adv. Electron. Mater.*, 2021, **7**, 2100043.
25 R. M. Cardoso, C. Kalinke, R. G. Rocha, P. L. dos Santos, D. P. Rocha, P. R. Oliveira, B. C. Janegitz, J. A. Bonacin, E. M. Richter and R. A. A. Munoz, *Anal. Chim. Acta*, 2020, **1118**, 73–91.
26 S. C. Daminabo, S. Goel, S. A. Grammatikos, H. Y. Nezhad and V. K. Thakur, *Mater. Today Chem.*, 2020, **16**, 100248.
27 J. S. Stefano, C. Kalinke, R. G. da Rocha, D. P. Rocha, V. A. O. P. da Silva, J. A. Bonacin, L. Angnes,

E. M. Richter, B. C. Janegitz and R. A. A. Muñoz, *Anal. Chem.*, 2022, **94**, 6417–6429.
28 T. D. Ngo, A. Kashani, G. Imbalzano, K. T. Q. Nguyen and D. Hui, *Composites, Part B*, 2018, **143**, 172–196.
29 E. M. Richter, D. P. Rocha, R. M. Cardoso, E. M. Keefe, C. W. Foster, R. A. A. Munoz and C. E. Banks, *Anal. Chem.*, 2019, **91**, 12844–12851.
30 S. V. F. Castro, A. P. Lima, R. G. Rocha, R. M. Cardoso, R. H. O. Montes, M. H. P. Santana, E. M. Richter and R. A. A. Munoz, *Anal. Chim. Acta*, 2020, **1130**, 126–136.
31 C. Kalinke, N. V. Neumsteir, P. Roberto de Oliveira, B. C. Janegitz and J. A. Bonacin, *Anal. Chim. Acta*, 2021, **1142**, 135–142.
32 A. Abdalla, H. H. Hamzah, O. Keattch, D. Covill and B. A. Patel, *Electrochim. Acta*, 2020, **354**, 136618.
33 R. Gusmão, M. P. Browne, Z. Sofer and M. Pumera, *Electrochem. Commun.*, 2019, **102**, 83–88.
34 C. Kalinke, N. V. Neumsteir, G. de O. Aparecido, T. V. de B. Ferraz, P. L. dos Santos, B. C. Janegitz and J. A. Bonacin, *Analyst*, 2020, **145**, 1207–1218.
35 E. G. Gordeev, A. S. Galushko and V. P. Ananikov, *PLoS One*, 2018, **13**, e0198370.
36 H. H. Bin Hamzah, O. Keattch, D. Covill and B. A. Patel, *Sci. Rep.*, 2018, **8**, 9135.
37 J. S. Stefano, L. R. Guterres e Silva, R. G. Rocha, L. C. Brazaca, E. M. Richter, R. A. Abarza Muñoz and B. C. Janegitz, *Anal. Chim. Acta*, 2022, **1191**, 339372.
38 V. Katseli, A. Economou and C. Kokkinos, *Talanta*, 2020, **208**, 120388.
39 V. A. O. P. Silva, W. S. Fernandes-Junior, D. P. Rocha, J. S. Stefano, R. A. A. Munoz, J. A. Bonacin and B. C. Janegitz, *Biosens. Bioelectron.*, 2020, **170**, 112684.
40 D. P. Rocha, A. L. Squissato, S. M. da Silva, E. M. Richter and R. A. A. Munoz, *Electrochim. Acta*, 2020, **335**, 135688.
41 R. G. Rocha, R. M. Cardoso, P. J. Zambiazi, S. V. F. Castro, T. V. B. Ferraz, G. de O. Aparecido, J. A. Bonacin, R. A. A. Munoz and E. M. Richter, *Anal. Chim. Acta*, 2020, **1132**, 1–9.
42 J. G. Walters, S. Ahmed, I. M. Terrero Rodríguez and G. D. O'Neil, *Electroanalysis*, 2020, **32**, 859–866.
43 A. Ambrosi, J. G. S. Moo and M. Pumera, *Adv. Funct. Mater.*, 2016, **26**, 698–703.
44 K. Y. Lee, A. Ambrosi and M. Pumera, *Electroanalysis*, 2017, **29**, 2444–2453.
45 A. H. Loo, C. K. Chua and M. Pumera, *Analyst*, 2017, **142**, 279–283.
46 J. Muñoz and M. Pumera, *Chemelectrochem*, 2020, **7**, 3404–3413.
47 M. Elbadawi, J. J. Ong, T. D. Pollard, S. Gaisford and A. W. Basit, *Adv. Funct. Mater.*, 2021, **31**, 2006407.
48 H. W. Tan, Y. Y. C. Choong, C. N. Kuo, H. Y. Low and C. K. Chua, *Prog. Mater. Sci.*, 2022, **127**, 100945.
49 G. L. Goh, H. Zhang, T. H. Chong and W. Y. Yeong, *Adv. Electron. Mater.*, 2021, **7**, 2100445.
50 O.-S. Kwon, H. Kim, H. Ko, J. Lee, B. Lee, C.-H. Jung, J.-H. Choi and K. Shin, *Carbon*, 2013, **58**, 116–127.
51 A. Moya, G. Gabriel, R. Villa and F. Javier del Campo, *Curr. Opin. Electrochem.*, 2017, **3**, 29–39.
52 A. Hussain, N. Abbas and A. Ali, *Chemosensors*, 2022, **10**, 103.
53 A. Maurel, M. Courty, B. Fleutot, H. Tortajada, K. Prashantha, M. Armand, S. Grugeon, S. Panier and L. Dupont, *Chem. Mater.*, 2018, **30**, 7484–7493.
54 F. P. W. Melchels, J. Feijen and D. W. Grijpma, *Biomaterials*, 2010, **31**, 6121–6130.
55 J. Wang, A. Goyanes, S. Gaisford and A. W. Basit, *Int. J. Pharm.*, 2016, **503**, 207–212.
56 S. Zekoll, C. Marriner-Edwards, A. K. Ola Hekselman, J. Kasemchainan, C. Kuss, D. E. J. Armstrong, D. Cai, R. J. Wallace, F. H. Richter, J. H. J. Thijssen and P. G. Bruce, *Energy Environ. Sci.*, 2018, **11**, 185–201.
57 J. P. Kruth, X. Wang, T. Laoui and L. Froyen, *Assemb. Autom.*, 2003, **23**, 357–371.
58 C. Zhao, C. Wang, R. Gorkin, S. Beirne, K. Shu and G. G. Wallace, *Electrochem. Commun.*, 2014, **41**, 20–23.
59 J. A. Lewis, *Adv. Funct. Mater.*, 2006, **16**, 2193–2204.
60 K. Fu, Y. Wang, C. Yan, Y. Yao, Y. Chen, J. Dai, S. Lacey, Y. Wang, J. Wan, T. Li, Z. Wang, Y. Xu and L. Hu, *Adv. Mater.*, 2016, **28**, 2587–2594.
61 T. C. Cândido, D. N. Silva, M. M. Borges, T. G. Barbosa, S. O. Trindade and A. C. Pereira, *Analytica*, 2024, **5**, 552–575.
62 J. S. Stefano, L. R. G. e. Silva and B. C. Janegitz, *Microchim. Acta*, 2022, **189**, 414.
63 C. Kalinke, P. R. de Oliveira, N. V. Neumsteir, B. F. Henriques, G. de Oliveira Aparecido, H. C. Loureiro, B. C. Janegitz and J. A. Bonacin, *Anal. Chim. Acta*, 2022, **1191**, 339228.
64 S. Olivera, H. B. Muralidhara, K. Venkatesh, K. Gopalakrishna and C. S. Vivek, *J. Mater. Sci.*, 2016, **51**, 3657–3674.
65 A. Rodríguez-Panes, J. Claver and A. M. Camacho, *Materials*, 2018, **11**, 1333.
66 K. Gnanasekaran, T. Heijmans, S. van Bennekom, H. Woldhuis, S. Wijnia, G. de With and H. Friedrich, *Appl. Mater. Today*, 2017, **9**, 21–28.
67 C. W. Foster, H. M. Elbardisy, M. P. Down, E. M. Keefe, G. C. Smith and C. E. Banks, *Chem. Eng. J.*, 2020, **381**, 122343.
68 S. W. Kwok, K. H. H. Goh, Z. D. Tan, S. T. M. Tan, W. W. Tjiu, J. Y. Soh, Z. J. G. Ng, Y. Z. Chan, H. K. Hui and K. E. J. Goh, *Appl. Mater. Today*, 2017, **9**, 167–175.
69 S. K. Jain and Y. Tadesse, *Int. J. Nanosci.*, 2019, **18**, 1850026.
70 S. Shi, Y. Chen, J. Jing and L. Yang, *RSC Adv.*, 2019, **9**, 29980–29986.
71 J. P. Hughes, P. L. dos Santos, M. P. Down, C. W. Foster, J. A. Bonacin, E. M. Keefe, S. J. Rowley-Neale and C. E. Banks, *Sustain. Energy Fuels*, 2020, **4**, 302–311.
72 H. H. Hamzah, S. A. Shafiee, A. Abdalla and B. A. Patel, *Electrochem. Commun.*, 2018, **96**, 27–31.
73 R. K. Gautam and A. Verma, in *Microbial Electrochemical Technology*, ed. S. V. Mohan, S. Varjani and A. Pandey, Elsevier, 2019, pp. 451–483.

74 D. Y. Kim, J. W. Park, D. Y. Lee and K. H. Seo, *Polymers*, 2020, **12**, 2020.
75 E. Vaněčková, M. Bouša, Š. Nováková Lachmanová, J. Rathouský, M. Gál, T. Sebechlebská and V. Kolivoška, *J. Electroanal. Chem.*, 2020, **857**, 113745.
76 W. Ye, W. Wu, X. Hu, G. Lin, J. Guo, H. Qu and J. Zhao, *Compos. Sci. Technol.*, 2019, **182**, 107671.
77 L. Ge, Q. Hong, H. Li, C. Liu and F. Li, *Adv. Funct. Mater.*, 2019, **29**, 1904000.
78 M. Berber and I. H. Hafez, *Carbon Nanotubes: Current Progress of Their Polymer Composites*, BoD – Books on Demand, 2016.
79 E. Bernalte, K. K. L. Augusto, R. D. Crapnell, H. G. Andrews, O. Fatibello-Filho and C. E. Banks, *RSC Appl. Interfaces*, 2025, DOI: 10.1039/D4LF00368C.
80 N. M. Caldas, L. V. de Faria, A. G. Batista, A. O. Alves, S. C. Silva, D. A. Peixoto, E. Nossol, D. P. Rocha, F. S. Semaan, W. F. Pacheco and R. M. Dornellas, *Electrochim. Acta*, 2024, **504**, 144868.
81 E. Redondo and M. Pumera, *Appl. Mater. Today*, 2021, **25**, 101253.
82 E. Vlachou, A. Margariti, G. S. Papaefstathiou and C. Kokkinos, *Sensors*, 2020, **20**, 4442.
83 D. Roy, R. Singh, N. Chanda and S. Mandal, *J. Appl. Electrochem.*, 2024, DOI: 10.1007/s10800-024-02220-x.
84 C. Kokkinos, A. Economou, A. Pournara, M. Manos, I. Spanopoulos, M. Kanatzidis, T. Tziotzi, V. Petkov, A. Margariti, P. Oikonomopoulos and G. S. Papaefstathiou, *Sens. Actuators, B*, 2020, **321**, 128508.
85 E. Koukouviti, A. K. Plessas, V. Pagkali, A. Economou, G. S. Papaefstathiou and C. Kokkinos, *Microchim. Acta*, 2023, **190**, 274.
86 B. Rezaei, J. Y. Pan, C. Gundlach and S. S. Keller, *Mater. Des.*, 2020, **193**, 108834.
87 M. A. Haque, N. V. Lavrik, A. Hedayatipour, D. Hensley, D. P. Briggs and N. McFarlane, *J. Vac. Sci. Technol. B*, 2020, **38**, 052203.
88 C. Yang, Q. Cao, P. Puthongkham, S. T. Lee, M. Ganesana, N. V. Lavrik and B. J. Venton, *Angew. Chem., Int. Ed.*, 2018, **57**, 14255–14259.
89 Y. Chang, Q. Cao and B. J. Venton, *Curr. Opin. Electrochem.*, 2023, **38**, 101228.
90 Q. Cao, M. Shin, N. V. Lavrik and B. J. Venton, *Nano Lett.*, 2020, **20**, 6831–6836.
91 Z. Shao, H. Zhao, K. E. Dunham, Q. Cao, N. V. Lavrik and B. J. Venton, *Angew. Chem.*, 2024, **136**, e202405634.
92 Y. S. Mutz, D. do Rosario, L. R. G. Silva, D. Galvan, J. S. Stefano, B. C. Janegitz, D. A. Weitz, P. C. Bernardes and C. A. Conte-Junior, *Food Chem.*, 2023, **403**, 134411.
93 T. P. Lisboa, L. V. de Faria, W. B. V. de Oliveira, R. S. Oliveira, M. A. C. Matos, R. M. Dornellas and R. C. Matos, *Microchim. Acta*, 2023, **190**, 310.
94 L. A. Pradela-Filho, D. A. G. Araújo, V. N. Ataide, G. N. Meloni and T. R. L. C. Paixão, *Anal. Bioanal. Chem.*, 2024, **416**, 4679–4690.
95 V. Katic, P. L. dos Santos, M. F. dos Santos, B. M. Pires, H. C. Loureiro, A. P. Lima, J. C. M. Queiroz, R. Landers, R. A. A. Muñoz and J. A. Bonacin, *ACS Appl. Mater. Interfaces*, 2019, **11**, 35068–35078.
96 H. A. Silva-Neto, M. Santhiago, L. C. Duarte and W. K. T. Coltro, *Sens. Actuators, B*, 2021, **349**, 130721.
97 M. P. Browne, F. Novotný, Z. Sofer and M. Pumera, *ACS Appl. Mater. Interfaces*, 2018, **10**, 40294–40301.
98 A. Fontana-Escartín, S. Lanzalaco, O. Bertran and C. Alemán, *Appl. Surf. Sci.*, 2022, **597**, 153623.
99 J. F. Hernández-Rodríguez, M. G. Trachioti, J. Hrbac, D. Rojas, A. Escarpa and M. I. Prodromidis, *Anal. Chem.*, 2024, **96**, 10127–10133.
100 M. El Fazdoune, K. Bahend, M. Oubella, S. Ben Jadi, A. El Guerraf, E. A. Bazzaoui, F. J. García-García, J. I. Martinis and M. Bazzaoui, *J. Polym. Environ.*, 2024, **32**, 2105–2119.
101 T. Takano, H. Masunaga, A. Fujiwara, H. Okuzaki and T. Sasaki, *Macromolecules*, 2012, **45**, 3859–3865.
102 M. Liao, Y. Yang, J. Ou, H. Yang, X. Dai, L. Zhong, J. Wen, Y. Jiang and L. Wang, *Electrochem. Commun.*, 2024, **165**, 107754.
103 M. Salve, A. Mandal, K. Amreen, P. K. Pattnaik and S. Goel, *Microchem. J.*, 2020, **157**, 104973.
104 N. Singh, H. Siddiqui, M. Goswami, S. Kumar, M. Ashiq, N. Sathish, M. S. Santosh and S. Kumar, *ACS Appl. Nano Mater.*, 2023, **6**, 3303–3311.
105 R. M. Cardoso, S. V. F. Castro, M. N. T. Silva, A. P. Lima, M. H. P. Santana, E. Nossol, R. A. B. Silva, E. M. Richter, T. R. L. C. Paixão and R. A. A. Muñoz, *Sens. Actuators, B*, 2019, **292**, 308–313.
106 M. Angelopoulou, D. Kourti, M. Mertiri, P. Petrou, S. Kakabakos and C. Kokkinos, *Chemosensors*, 2023, **11**, 475.
107 A. Rivas-Macho, U. Eletxigerra, R. Diez-Ahedo, S. Merino, A. Sanjuan, M. M. Bou-Ali, L. Ruiz-Rubio, J. del Campo, J. L. Vilas-Vilela, F. Goñi-de-Cerio and G. Olabarria, *Heliyon*, 2023, **9**(1), e12637.
108 G. Martins, J. L. Gogola, L. H. Budni, B. C. Janegitz, L. H. Marcolino-Junior and M. F. Bergamini, *Anal. Chim. Acta*, 2021, **1147**, 30–37.
109 S. Malhotra, D. S. Pham, M. P. H. Lau, A. H. Nguyen and H. Cao, *Sensors*, 2022, **22**, 2382.
110 J. Muñoz and M. Pumera, *Chem. Eng. J.*, 2021, **425**, 131433.
111 C. E. C. Lopes, L. V. de Faria, D. A. G. Araújo, E. M. Richter, T. R. L. C. Paixão, L. M. F. Dantas, R. A. A. Muñoz and I. S. da Silva, *Talanta*, 2023, **259**, 124536.
112 T. P. Lisboa, G. F. Alves, L. V. de Faria, C. C. de Souza, M. A. C. Matos and R. C. Matos, *Talanta*, 2022, **247**, 123610.
113 R. Domingo-Roca, P. Lasserre, L. Riordan, A. R. Macdonald, A. Dobrea, K. R. Duncan, S. Hannah, M. Murphy, P. A. Hoskisson and D. K. Corrigan, *Biosens. Bioelectron.:X*, 2023, **13**, 100308.
114 T. T. Do, H. Van Giap, M. T. T. Nguyen, D. T. Hoang, H. L. Nguyen, L. T. Le, L. D. Tran and D. T. Nguyen, *Colloid Polym. Sci.*, 2023, **301**, 1029–1038.

115 Jyoti, E. Redondo, O. Alduhaish and M. Pumera, *Electroanalysis*, 2023, **35**, e202200047.
116 X. Wei, C. Liu, X. Zhang, Z. Li, X. Wang, Y. Xu, J. Shi, Q. Sun, M. N. Routledge, D. Zhang and X. Zou, *Sens. Actuators, B*, 2023, **376**, 132941.
117 M. F. Santangelo, I. Shtepliuk, D. Filippini, D. Puglisi, M. Vagin, R. Yakimova and J. Eriksson, *Sensors*, 2019, **19**, 2393.
118 J.-H. Shin, K.-D. Seo, H. Park and D.-S. Park, *Electroanalysis*, 2021, **33**, 1707–1714.
119 A. Baltima, H. Panagopoulou, A. Economou and C. Kokkinos, *Anal. Chim. Acta*, 2021, **1159**, 338426.